CSUG/SPE 149190

Solvent Chamber Development in 3D Physical Model Experiments of Solvent Vapour Extraction Processes (SVX) With Various Permeabilities and Solvent Vapour Qualities

Kelvin D. Knorr, SPE, and Muhammad Imran, SPE, Saskatchewan Research Council

This paper was prepared for presentation at the Canadian Unconventional Resources Conference held in Calgary, Alberta, Canada, 15–17 November 2011.

Abstract

Solvent vapour extraction (SVX) processes offer an attractive alternative to thermal recovery processes, being less energy intensive; and are more suitable for thinner, partially depleted reservoirs. A typical SVX process uses solvent injection to dilute the heavy oil by reducing its viscosity, allowing it to be mobilized for production. During this process the injection of hydrocarbon solvents results in partial deasphalting of the heavy oil, thus further reducing its viscosity and enhancing the process performance.

This work examined the formation and growth of solvent chambers in laterally and vertically spaced horizontal injector/producer well pairs in porous media with five different permeabilities and three different solvent vapour qualities. Consolidation of the porous media due to asphaltene precipitation was also analyzed. Thermal imaging and model excavation studies were performed to investigate the formation and growth of solvent chambers for seven different experiments conducted on a large 3D physical model apparatus.

The important findings from this study are as follows: During solvent injection, one or more solvent fingers develop between the injector and producer. The dominant solvent finger becomes a conduit that grows into a solvent chamber connected to the injection well in the upper portion of the reservoir, and develops into an oil drainage conduit connected to the production well in the lower portion of the reservoir. Solvent dispersion layers are located on the margins of both the solvent chambers and the oil drainage conduits. The location and development of these non-uniform solvent chambers and oil drainage conduits are unpredictable, and the oil drainage conduits do not grow significantly in diameter once connected to the production wellbore, limiting the wellbore inflow efficiency and conformity. Asphaltene precipitation and migration can aggravate this inflow problem, further reducing SVX process performance.

SVX performance can be improved by increasing the number and diameter of oil drainage connections between the solvent chamber and the production well, and by controlling the oil deasphalting process. This can be done by optimizing injection and production wellbore geometries, and by optimizing solvent injection rates and vapour quality.

Introduction

Canada's western provinces are very rich in unconventional hydrocarbon oil reserves like heavy oil and bitumen. To keep up with existing and future world energy demands we need to utilize these types of reservoirs. The exploitation of these reservoirs is somewhat problematic, with low recoveries of the original oil in place (OOIP). Although some enhanced oil recovery processes like steam-assisted gravity drainage, cyclic steam stimulation, and in-situ combustion are being implemented to extract this oil, application of these thermal processes is limited to thicker reservoirs and is very energy intensive. One group of technologies showing good promise are solvent vapour extraction (SVX) processes, which include a number of solvent injection methods for both horizontal and vertical wells (Kristoff et al. 2008).

SVX processes use solvent injection to dilute the heavy oil, allowing it to be mobilized. Binary mixtures of methane or carbon dioxide carrier gas with propane or butane solvents are currently the best candidates for injection. Unlike thermal EOR processes, SVX is a low energy, non-thermal process that generates little greenhouse gases.

Lateral SVX processes are similar to the Vapex process (Butler and Mokrys 1991) except for the difference in injection and production well arrangements. For a typical lateral SVX process the injection and production wells are both vertically and laterally

(horizontally) spaced. This well arrangement is useful for application in thinner reservoirs (Butler and Jiang 2000). Upon solvent injection, a solvent chamber develops between the injection and production wells. A thin transition layer is formed at the edge of this solvent chamber. At one side of this layer, the solvent is at its maximum concentration; it disperses into the oil, resulting in an oil viscosity reduction, and may cause the partial precipitation of the asphaltenes from the oil (Upreti et al. 2007). Due to the dissolution process, different oil viscosities exist in each layer within the interface thickness. Once the viscosity of the oil is sufficiently reduced, the diluted oil starts to drain to the production well by gravity and by whatever small pressure differentials may be present. Once a layer of reduced viscosity oil is drained, the solvent dissolution process continues with the next layer of oil with higher viscosity, thus resulting in an expansion of the solvent chamber and the movement of the oil/solvent interface. During SVX processes, solvent dissolution results in a temperature increase at the oil/solvent interface. This effect is described by Dunn et al. (1989) who investigated dispersion in a 2D model using carbon dioxide and ethane with Athabasca bitumen. The authors estimated that temperature changes of 2 to 4°C might occur at this interface. This has been confirmed in this work, in which these small temperature changes have been used to image solvent movement in the 3D physical models.

In SVX processes, solvents in their pure form or their mixtures with non-condensable gases are injected close to their dewpoint pressure. The injection of vaporized solvents near their dewpoint results in partial deasphalting of the oil that offers additional viscosity reduction beyond that by dilution, which further promotes the oil production rate (Das and Butler 1998). However, injection of solvent above the dewpoint pressure (two-phase region) for significant periods of time may result in extensive asphaltene precipitation that can cause plugging of the pores as well as of the diluted oil drainage pathway, reducing oil production rates and recoveries.

Many researchers have investigated solvent-based recovery processes to identify production stages and to evaluate the dependence of oil production rates and recoveries on such reservoir properties as drainage height and reservoir permeability. Das and Butler (1999) identified four production stages for these processes that include downward displacement of oil, initial solvent chamber formation, constant or nearly constant oil production rate during solvent chamber expansion, and the solvent chamber reaching lateral boundaries with a subsequent decrease in oil production rates. Jiang and Butler (1995), Oduntan et al. (2001), and El-Haj et al. (2009) investigated the recovery process dependence on reservoir permeabilities over a limited range. Most of the investigations during the last two decades have been conducted with 2D physical models and exaggerated permeabilities. Only a few studies have been performed with field type permeabilities due to long experiment durations measured in months, rather than hours (Sim and Singhal 2002). None of these investigations included the 3D aspect of SVX processes with field type permeabilities. The formation of the solvent chamber(s) and the recovery mechanism differs for a 3D model with field type permeabilities compared to a 2D model with much higher permeabilities.

This work examined the formation and growth of solvent chambers in lateral SVX processes with five different permeabilities ranging from approximately 4 to 3,000 μm^2 (darcies) and three different solvent vapour qualities. Seven experiments were performed in large 3D physical models of two different sizes. The initial dead oil viscosity ranged from 5,000 to 6,000 mPa·s at 27°C. A 14/86 mole percent mixture of CH_4/n-C_4H_{10} was used as the injected solvent. For two of the runs the injected solvent vapour quality was varied to evaluate the effect of two-phase injection. The solvent chamber development and growth were imaged using temperature data from a uniform grid of thermocouples installed within the 3D model. At the end of the experiments, the 3D models were excavated and photographed to study the asphaltene precipitation streaks, residual oil saturations, solvent chamber/conduit locations and shapes, and the connections to the horizontal production well.

Experimental Setup and Procedures

The large 3D scaled physical model apparatus installed at SRC's Regina laboratories was used to conduct seven SVX experiments. A schematic of the experimental setup is shown in **Fig. 1. Fig. 2** shows the high-pressure vessel with a 3D physical model inside. The safe design and operational considerations, and facility and equipment specifications are described elsewhere (Knorr et al. 2008).

The experiments were conducted in a tub and lid–style box model with 100-cm injection and production wells that were laterally and vertically separated along the width and height of the model. For the first two runs, i.e., SVX 1 and 2, the height and width of the model was shortened such that the model had L×W×H of 100×26×27 cm. The rest of the experiments were performed with L×W×H of 100×50×51 cm. Potters glass beads were used to pack the physical models homogeneously. Five different size ranges representing five different permeabilities were used in the seven experimental runs. A modified Carman-Kozeny correlation given by Panda and Lake (1994) was used along with core displacement tests to determine the absolute or single-phase permeability of the homogeneous packing material. All these experiments were performed at the model/reservoir temperature of 27°C. The solvent injection pressure for these runs was varied to inject the solvent mixture at the desired vapour quality. **Table 1** shows the average injection pressure, model dimensions and properties of the porous media.

The 3D physical models were equipped with a grid of 90 thermocouples to image the solvent vapour movement inside the model as well as the development of solvent chambers. For the larger model experiments (SVX 3 to 7), all 90 thermocouples were utilized inside the model, whereas for the smaller models (SVX 1 and 2) only 36 thermocouples were used. **Fig. 3** shows the uniform thermocouple grid in the rectangular models. The dotted lines in the figure present the smaller model size.

All of these experiments were performed with three oil recovery stages. During the first stage, oil was recovered by injecting water at high rates (waterflood). During the second stage, oil was recovered by injecting a mixture of methane gas and normal butane solvent (SVX). During the third stage, oil was recovered with scheduled pressure reductions in the model (blowdown).

The preparation and operation of the seven experiments were made as consistent as possible except for the change in permeability, model dimensions and injection pressure (vapour quality). Once the wells, thermocouples and other ports were secured in the model, glass beads were vibrated into place and the lid was sealed. The model was then evacuated and imbibed with deionized water to determine the pore volume (PV). The model was slid into the overburden pressure vessel, which was then sealed and filled with warm water to heat the model to the oil injection temperature. An overburden pressure differential of at least 50 kPa was established with a model pressure of ~500 kPaa.

Heavy oil with an initial dead oil viscosity ranging from 5,000 to 6,000 mPa·s at 27°C was used for the oil phase. For each run, the oil was injected into the top horizontal well at elevated temperatures ranging from 45 to 55°C for ~1.5 to 1.6 pore volumes to resaturate the model to residual water saturation. The oil injection phase lasted between 3 and 35 hours for the seven runs, with the longer times required for the lower permeability and larger models.

The temperature of the model was reduced to ~27°C, and waterflooding was conducted to reduce the initial oil saturation to more field-like values, and to provide injectivity for the subsequent solvent injection. Deionized water was injected for ~1.4 pore volumes at which point the produced water cut was ~97 to 98%. After waterflooding, the backpressure of the horizontal production well was set in the range of 300 to 400 kPaa, with different injection pressures resulting in different solvent vapour qualities, and the temperature was maintained close to 27°C. A mixture of 14/86 mol percent of methane and n-butane was used as the solvent. A Peng-Robinson (1976) equation of state (EOS) simulator was used to determine the required composition and quality of the injected solvent mixture, as well as the thermodynamic properties. The solvent injection rates for all seven experiments were very similar, ranging from 0.806 kg/hr to 0.813 kg/hr. The solvent injection continued until the production declined or a problem occurred. After solvent injection was completed, the model was blown down based on scheduled pressure reductions followed by a production period while the model pressure stabilized. Once atmospheric pressure was reached, the model lid was removed and allowed to degas overnight. The model was then excavated in depth intervals resulting in five to six layers. Each layer was photographed to study the asphaltene precipitation streaks, residual oil saturations, solvent chamber/conduit locations and shapes, and the connections to the horizontal production well.

Results and Discussion

Waterflood and Solvent Injection Results.

As mentioned earlier, an initial waterflood phase was performed for all seven runs to reduce the oil saturation to more field-like values and to provide injectivity for solvent injection. **Table 2** summarizes the waterflood details, including waterflood time, initial and final oil and water saturations, and oil recovery in litres and %OOIP. The initial water saturations were higher for the smaller models with higher permeabilities. The waterflood %OOIP recovery was higher for larger models with lower permeabilities. The run with the highest permeability recovered the least amount of oil during waterflooding because of early water fingering and breakthrough due to the high permeability.

Table 3 presents the solvent injection time, initial and final model saturations for oil, water and gas, solvent retention in the model as a percent of the injected solvent mass, and oil production rate and recovery in litres/day and %OOIP. The actual solvent injection times for these runs were longer and oil recoveries were higher than what is presented in Table 3. For comparative purposes the results in this table are presented for an equal amount of solvent injected/pore volume, i.e., the solvent injection times correspond to 0.212 kg of solvent injected per litre of pore volume. The highest permeability model achieved the highest oil recovery and the highest oil production rate (SVX 1). Of the two models with the same permeability and different model heights and widths (SVX 2 and 3), the model with the larger height and width achieved a slightly higher oil recovery and production rate, that is, 29.4% OOIP compared to 26.6% OOIP with a rate of 25.3 litre/day compared to 20.8 litre/day.

During these seven experiments, the vapour quality of the injected solvent was varied. Specifically for SVX 5 and 6, the solvent mixture was injected well above the dewpoint pressure that resulted in the injection of solvent in the two-phase region for ~37% of the injection time for SVX 5 and ~100% of the injection time for SVX 6. This resulted in an averaged solvent vapour quality of ~85% for SVX 5 and ~50% for SVX 6. For the remaining runs, the solvent vapour quality was ~100% vapour. Comparison of the results of the field type permeability models having the same model dimensions (i.e., SVX 5 to 7) indicates that oil and solvent recovery in SVX processes depends upon the solvent vapour quality. Injection of the solvent mixture at 100% vapour quality for long durations resulted in higher oil recoveries and production rates. SVX 7 produced the highest oil recovery among these three experiments.

Solvent retention in the model is an important aspect of SVX processes that needs to be minimized for optimized economics. This study showed that injection of the solvent in a two-phase region for longer times resulted in higher solvent retention in the model. Solvent was injected in the two-phase region for ~100% of the injection period in SVX 6, which had the highest solvent retention of any of the seven SVX experiments. **Table 4** shows the same run information as contained in Table 3, except that it includes data for the total run times.

Model Excavation and Thermal Imaging Results.

In this work thermal imaging and 3D model excavation studies were performed to investigate the formation and growth of solvent conduits and chambers for different permeability models. The models were excavated from the top in 5 to 9 cm intervals to obtain at least five layers for each SVX run. The photographs for each layer for every run were compiled for comparative purposes. The solvent chamber(s) and oil drainage conduits as well as asphaltene depositions were approximated from these photos by carefully viewing the colour distribution among these layers, and analyzing selected samples for oil, water, solids and asphaltenes. The shapes of the solvent chambers were also approximated by imaging the temperature changes in the model during the solvent injection.

As the solvent contacts the heavy oil, the thermocouple grid measures the small temperature increases due to the dissolving solvent, and thermal images of the solvent injection process can be generated from this information. This provides an indirect observation of solvent movement, as well as of the growth of the solvent chamber within the model. The maximum temperature images indicate all the regions where solvent was present at some period during the solvent injection, and the extent of the solvent chamber development. Just as important are the regions where no temperature changes were observed indicating no solvent contact.

Figs. 4 and 5 show the model excavation photographs and maximum temperatures recorded during the solvent injection phase of SVX 1. The total solvent injection time for this run was 6.98 hours, and it recovered 51.3% OOIP with an average oil production rate of 41.7 litres/day. SVX 1 had the highest permeability of 2,960 μm^2. The upper layers of this run were cleaned to low residual oil saturations, with asphaltene deposits observed near the chamber boundaries. The maximum temperature plot showed that the full length of injection well was involved in formation of a solvent chamber that was connected to the production well. No wellbore conformity issues were observed from the thermal images. The solvent chamber was well developed across the whole model within ~7 hours of solvent injection.

Figs. 6 and 7 show the model excavation photographs and maximum temperatures recorded during the solvent injection phase of SVX 2. The total solvent injection time for this run was 6.94 hours; it recovered 27.6 % OOIP with an average oil production rate of 20.8 litres/day. SVX 2 had a permeability of 301 μm^2, which was approximately ten times less than that of SVX 1. Similar to SVX 1, the upper layers were cleaned to very low residual oil saturations of less than 5% of the pore volume. The asphaltene deposits in this run were observed close to the injection and production wells, as well as at the solvent/oil interface. The maximum temperature plot showed the presence of a well-developed solvent chamber at both top corners of the model, with a partially developed solvent chamber near the middle of the model.

Figs. 8 and 9 show the model excavation photographs and maximum temperatures recorded during the solvent injection phase of SVX 3. The total solvent injection time for SVX 3 was 68.2 hours compared to ~7 hours for SVX 1 and 2. The longer injection time resulted in a higher %OOIP recovery of 64.8% OOIP, with an average oil production rate of 19.8 litres/day. This run had a permeability of 301 μm^2, which was the same as in SVX 2. The higher recovery resulted in lower residual oil saturation in all five layers. Similar to SVX 2 the asphaltene deposits were observed close to the injection and production wells and solvent/oil interface. During the excavation of this model, a very distinct solvent/oil interface was captured and is presented in **Fig. 10**. A close analysis of Fig. 10 shows that closest to the solvent chamber boundary, the residual oil is light brown or tan coloured, and it becomes increasingly darker brown towards the unaffected black oil. A precipitated asphaltene layer lies on top of an amber brown layer before graduating to the black oil. The thickness from the solvent chamber to the black oil is ~5 cm. The maximum temperature plot for this run shows a well-developed solvent chamber formed within 40% of the model, producing the oil by direct contact of the solvent chamber to the production well. In the remaining 60% of the model, the solvent chambers were partially developed and the oil was produced through oil drainage conduits connected to the production well.

Figs. 11 and 12 show the model excavation photographs and maximum temperatures recorded during the solvent injection phase of SVX 4. The total injection time for this run was 65.6 hours; it recovered 22.9% OOIP with an average oil production rate of 7.2 litres/day. SVX 4 was performed with a permeability of 30 μm^2. The top layer of this run was cleaned to very low residual oil saturation. An anomalous region of higher oil saturation was observed in the middle of the second layer. Because of the lower oil recovery, the oil saturation in layers 3 to 5 was high. The maximum temperature plots showed the presence of a well-developed solvent chamber within ~20% of the model, contacting the production well directly. In the remaining 80% of the model, partially developed solvent chambers were observed in the top layers, and were connected to the production well through oil drainage conduits.

Figs. 13 and 14 show the model excavation photographs and maximum temperatures recorded during the solvent injection phase of SVX 5. The total solvent injection time for this run was 42.9 hours; it resulted in 24.5% OOIP recovery with an average oil production rate of 12.0 litres/day. SVX 5 was performed with a permeability of ~9 μm^2. During this run, the solvent mixture was injected in the two-phase region for a certain time period, i.e., partial vapour and partial liquid injection. Compared to the previous runs, asphaltene precipitation was more severe and deposits were observed within all five layers of the model. Asphaltene migration was so extensive that the solvent injection was stopped early due to plugging of the production line. The excavation photographs of this run show the formation of a large lateral chamber that connects to the production chamber through an oil drainage conduit (as shown in layers 4 and 5). The oil drainage conduit was very small compared to the solvent chamber. The photographs also show that a funnel formed at the junction of the oil drainage conduit and solvent chamber (as shown in layers 2 and 3), due to the size difference between the solvent chamber/solvent conduit and oil drainage conduit. Such funnels can restrict the rate of oil drainage from the solvent chambers. More than one oil drainage

conduit was observed in this run. The maximum temperature plots of this run showed the presence of a fully developed solvent chamber in the middle of the model that expanded laterally. The remaining model had partially developed solvent chambers with limited connectivity to the production well, resulting in poor wellbore conformance/efficiency.

Figs. 15 and 16 show the model excavation photographs and maximum temperatures recorded during the solvent injection phase of SVX 6. The total solvent injection time for this run was 108 hours; it had a net recovery of 29.6% OOIP and an average oil production rate of 5.8 litres/day. SVX 6 was performed with a permeability of ~4 μm^2. The injection in this run was stopped prematurely due to plugging of the matrix and the production lines. This occurred due to extensive asphaltene precipitation and migration caused by solvent injection in the two-phase region for 100% of the injection time. Asphaltene streaks were observed throughout the whole model. Connection of the solvent chamber to the production well was through an oil drainage conduit (as shown in layer 5). The maximum temperature plots show the presence of a partially developed solvent chamber across 60% of the injection well length. The oil drainage conduits, although difficult to see, connect to only 20 to 30% of the production well length.

Figs. 17 and 18 show the model excavation photographs and maximum temperatures recorded during the solvent injection phase of SVX 7. The total solvent injection time for this run was 202 hours; it had a net recovery of 62.2% OOIP and an average oil production rate of 6.5 litres/day. SVX 7 was performed with a permeability of ~4 μm^2, the same as in SVX 6. The excavated layers show clean porous media with very low residual oil saturations within ~ 90% of the model. The highest oil saturations were found in the bottom layer close to the production well. Some asphaltene streaks were found in all layers; however, the asphaltene precipitation was not as massive as observed in SVX 6 and SVX 5. Limited asphaltene migration did not cause excessive plugging in the matrix or the production lines. The significant amount of cleaned porous media near the production well in layer 6 showed that nearly 100% of the production well was connected to solvent chambers or associated oil drainage conduits, resulting in very good production wellbore conformity/efficiency. The time-dependent temperature plots showed that multiple solvent chambers formed, expanded and developed drainage conduits across the whole production wellbore length. The maximum temperature plot shows the endpoint of this process.

The above analysis of the model excavation photographs and thermal images of the seven runs revealed that the recovery mechanism in these SVX runs started from the formation of a solvent conduit(s). **Fig. 19** presents a stepwise mechanism showing the development of the solvent conduits, solvent chambers, oil drainage conduits and the effects on wellbore conformity/efficiency at six different cumulative times from the start of solvent injection. Solvent conduits develop along the water channels or solvent fingers connecting the injection and production wells in the very early solvent injection times (T_1). Often more than one finger will develop into solvent conduits, but one or two will eventually dominate (T_2). Solvent fingering with one finger becoming dominant has been previously described by Cuthiell et al. (2003). At both of these early times, the connection to the injection or production wells is limited, and the wellbore conformity is poor. A significant solvent vapour flux travels in both the radial and length directions in the conduits. This is due to concentration gradients (radial) and pressure gradients (length). A solvent dispersion layer forms on the walls of the conduit where oil dilution and viscosity reduction occur until a thin layer of diluted oil drains away, exposing a less diluted oil layer.

The draining of the diluted oil from the dispersion layer on the conduit walls results in the widening of solvent conduit until the internal diameter is sufficient to allow free solvent vapour to flow at low velocities. Further widening of solvent conduit slows but continues as it converts into a solvent chamber in the upper portions of the model. The growth and ultimate size of the first solvent chamber are unpredictable, and often other water channels or solvent fingers receive sufficient solvent flows such that they develop into conduits and later into solvent chambers as well. In addition, adjacent solvent chambers often merge, with improvements in both injection and production wellbore conformity/efficiency (T_3 and T_4). As the solvent conduits develop into solvent chambers and oil drainage conduits, the oil production rate is semi-stabilized and the wellbore conformity improves. The injection well conformity improves faster than the production well conformity. The merged solvent chambers continue to expand along the injection well and between the injection and production wells (T_5 and T_6). Wellbore conformity continues to improve until the oil production rate begins to decline, at which point the growth in the production well conformity stalls.

Figs. 20 and 21 shows the likely concentration gradients present in the solvent and oil drainage conduits. In a solvent conduit, the solvent concentration gradient in the radial direction is much larger than in the length direction. This results in a radial expansion of the solvent conduit into a solvent chamber connected to the injection well in the upper portion of the model. Whereas solvent conduits have large radial concentration gradients, oil drainage conduits have small radial concentration gradients, due to the difference between the conduits being filled with solvent vapour versus diluted oil. Correspondingly, solvent conduits have small concentration gradients along their length due to the flowing solvent vapour phase, while oil drainage conduits have larger concentration gradients along their length, with greater oil dilution near the transition between a solvent conduit and an oil drainage conduit. Because of the low radial concentration gradient, oil drainage conduits do not widen very fast and therefore do not grow much along the length of the production well with time. This limits the wellbore conformity/efficiency.

As solvent diluted oil drains from the margins of the solvent conduits and solvent chambers, the lower sections of the conduits become oil drainage conduits connected to the production well in the lower portion of the model. The growth rate of the solvent chamber(s) depends upon the size and number of oil drainage conduits that link the production well with the solvent chambers. As with solvent chambers, the location and development of these non-uniform oil drainage conduits are unpredictable.

The unlimited radial growth of the solvent conduit into a solvent chamber at the top of the model, combined with the limited growth of the oil drainage conduits in the radial direction, generates a funnel, where the top of the solvent conduit connecting to the solvent chamber is large, while the bottom connecting to the production well is small. In general, once a solvent chamber is sufficiently developed, more diluted oil is capable of draining than can be accommodated with the oil drainage conduit, and this restrictive funnel effect becomes the oil-production-rate-limiting mechanism in the process. The funnel effect can result in a straight-line oil production curve with a plateau after most of the oil has been produced. In SVX processes where the production of diluted oil in not hindered by the funnel effect, i.e., sufficient oil drainage conduits are connected to the production well, the oil production curve is more 'S shaped.' **Fig. 22** shows a comparison of possible oil production curves with and without a restrictive funnel effect. The S shaped curve results from an initial period when the solvent/oil contact area increases slowly along with the establishment of many oil drainage conduits. This is followed by the rapid growth in the solvent/oil contact area and a corresponding rapid oil production period. Eventually the rate begins to decrease again as most of the oil has been produced.

The funnel effect and wellbore conformity/efficiency related to oil drainage conduits is more pronounced for lower permeability models. In high permeability models, the solvent chamber or solvent conduit is in direct contact with the production well across most or all of the well length. That provides for the maximum drainage paths for the diluted oil to be produced and results in a higher production rate and near 100% injection and production well efficiency. In low permeability models, the solvent chamber is connected to the production well through one or more diluted oil drainage conduit(s). The bottom of the conduit (funnel) fills with slower draining diluted oil from the solvent chamber. This results in a limited number of drainage paths for the diluted oil to be produced and results in a lower overall production rate and production well efficiency.

Injection of solvents with less than 100% vapour quality (i.e., some liquid solvent phase) results in extensive asphaltene precipitation, especially near the injection well and the solvent/oil interfaces. These asphaltenes can cause partial consolidation and plugging of the porous media. This reduction in porosity does not significantly restrict the solvent inflow around the injection well due to the very low viscosity of the solvent vapour. However, these asphaltenes can migrate with the diluted oil into the oil drainage conduits, where porosity reductions can significantly aggravate the funnel effect by further restricting the oil drainage rate between the solvent chamber and the production well. In addition, reducing the diluted oil drainage rate can also restrict the growth of oil drainage conduits in both length and radial directions, thus reducing the production wellbore conformity/efficiency even further.

A number of possible ways to improve the solvent chamber drainage and production well conformity/efficiency have been considered. They all attempt to address the funnel effect by increasing the number, size, or the efficiency of the oil drainage conduits between the solvent chamber and the production wellbore:

1) Reduce the funnel effect by directly increasing the number of oil drainage conduits for efficiency by drilling reduced diameter multilateral wellbores from the horizontal production well towards the injection well. These multilateral wellbores can be left open-hole, since even if they partially collapse (in unconsolidated media) the increased permeability can still provide significant additional drainage pathways between the solvent chamber and the production well.

2) Improve the mobility of the oil adjacent to the production well. The radial growth of the oil drainage conduits is restricted by the low mobility (high viscosity) of the oil surrounding these conduits. The most direct method to accomplish this is to reduce the oil viscosity near the production well either through solvent or thermal stimulation. This can improve the number of connections between the solvent chamber and the wellbore, improving the wellbore conformity and increasing the oil production rate.

3) Reduce the asphaltene precipitation and migration by injecting the solvent in a 100% vapour region. This approach can reduce the amount of conduit plugging, and maintain the highest possible drainage efficiency, wellbore conformity and diluted oil production rate of whatever conduits are available.

4) Increase the solvent injection rate, as long as care is taken to avoid excess solvent injection, which can lead to undesirable solvent storage or losses in the reservoir. An increased solvent injection rate can provide two benefits for improving the solvent chamber drainage rate. Firstly, it can lead to more solvent fingers connecting the injection and production wells, which subsequently become solvent chambers and drainage conduits. Secondly, the increased rate can also develop higher pressures gradients between injection and production wells, which can add a complementary driving force for oil production along with the usual gravity drainage mechanism. These gradients reduce with time as the solvent chamber(s) grow and the compressibility of the solvent vapour tends to dampen pressure changes.

5) Drill open-hole multilateral wellbores reaching from the injection well towards the production well. This would facilitate controlled and directional solvent fingering to occur during the initial solvent injection period, before substantial solvent breakthrough to the producing well occurs and new solvent fingering is effectively stopped. Ideally, at least one, and hopefully more, solvent conduit(s) would develop between each multilateral wellbore and the producing wellbore. These solvent conduits would develop into multiple oil drainage conduits, which may connect to each other and grow radially, thus reducing/eliminating the funnel effect and improving the production wellbore efficiency and oil production rate.

Conclusions

This work examined the formation and growth of solvent chambers in an SVX process with five different permeabilities ranging from approximately 4 to 3,000 μm^2 and three different solvent vapour qualities. Seven experiments were performed in large 3D

physical models of two different sizes. The horizontal injection and production wells were separated both laterally and vertically. The experiments were performed with an initial dead oil viscosity ranging from 5,000 to 6,000 mPa·s at a temperature of 27°C. A 14/86 mole percent mixture of CH_4/n-C_4H_{10} was used as the injected solvent; the injected solvent vapour quality varied between 50 to 100% among the seven runs. In each run, prior to solvent injection, a waterflood was performed to reduce the oil saturation levels to more 'field-like' values, and to provide a suitable injectivity for solvent injection. A blowdown phase followed each solvent injection period. The injected solvent location and the solvent chamber(s) growth were imaged using temperature data from a uniform grid of thermocouples installed within the 3D model. At the completion of the experiments, the 3D models were excavated and photographed to study the asphaltene precipitation streaks, residual oil saturations, solvent conduits, and solvent chamber(s) shape and location.

The oil recoveries and production rates during the solvent injection phase of all these runs were compared on the basis of equal amount of solvent injected per pore volume (0.212 kg of solvent injected/litre of pore volume). These results revealed that higher permeability models achieved the highest oil recovery and production rates, as was expected. Oil recovery and production rate were also enhanced by increased model/reservoir height, as shown by comparing runs with the same parameters except for different model dimensions. The results of the runs with poor solvent vapour quality showed that injection of a two-phase solvent mixture at the reservoir temperature (above its dewpoint pressure) negatively influenced the SVX recovery process due to extensive asphaltene precipitation that caused both porosity reductions and plugging of the production wells and lines.

The thermal imaging and model excavation studies showed that during solvent injection, one or more solvent chambers developed between the injector and producer. Such chambers—which tended to be smaller and less uniform in 'field type' permeability porous media—originated from solvent conduits that formed when the injected solvent initially followed water channels or fingers through the porous matrix from the injector to the producer, with the dominant finger or fingers becoming the conduits. In the upper portion of the reservoir, the solvent conduits developed into solvent chambers connected to the injection well, and in the lower portion of the reservoir, developed into oil drainage conduits connected to the production well. The location and development of these non-uniform solvent chambers and oil drainage conduits were unpredictable, and the oil drainage conduits did not grow significantly in diameter once connected to the production wellbore, limiting the wellbore inflow efficiency and conformity. Asphaltene precipitation and migration aggravated this inflow problem further reducing SVX process performance. The oil drainage conduits were much smaller compared to the solvent chambers; this resulted in a restrictive funnel effect that limited the production wellbore conformity/efficiency and, consequently, the diluted oil production rate. This funnel effect was more pronounced for low permeability models.

SVX performance can be improved by reducing the funnel effect by increasing the number and diameter of oil drainage conduits, improving the wellbore conformity, and consequently improving the oil production rates. This can be accomplished by adding open-hole multilateral wellbores between the horizontal injection and production wells, increasing the oil mobility adjacent to the production wells through solvent or thermal stimulation, optimizing solvent injection rates and strategies, and controlling the oil deasphalting process by maximizing solvent vapour quality.

Acknowledgements

This study was undertaken at SRC in support of the PTRC's multiclient EOR research program: Evaluation of Solvent Vapour Extraction (SVX) Processes Using a 3D Physical Model Year 1 and Year 2, and was conducted using a large 3D physical model, which is currently being operated at SRC's Regina laboratories to study solvent vapour extraction (SVX) processes.

References

Butler, R.M. and Jiang, Q. 2000. Improved Recovery of Heavy Oil by Vapex with Widely Spaced Horizontal Injectors and Producers. *J. Cdn. Pet. Tech.* **39** (1): 48–56.

Butler, R.M. and Mokrys, I.J. 1991. A New Process (Vapex) For Recovering Heavyn Oils Using Hot Water and Hydrocarbon Vapour. *J. Cdn. Pet. Tech.* **30**: 97–106.

Cuthiell, D., McCarthy, C., Frauenfeld, T., Cameron, S., and Kissel, G. 2003. Investigation of the Vapex Process Using CT Scanning and Numerical Simulation. *J. Cdn. Pet. Tech.* **42** (2): 41–49.

Das, S.K. and Butler, R.M. 1999. Investigation of Vapex Process in a Packed Cell Using Butane as Solvent. Paper presented at the 1999 CIM Annual Technical Conference, Calgary, 20–23 March.

Das, S.K. and Butler, R.M. 1998. Mechanism of the Vapour Extraction Process for Heavy Oil and Bitumen. *J. Pet. Sci. Eng.* **21** (1–2): 43–59.

Dunn, S.G., Nenniger, E.H., and Rajan, V.S.V. 1989. A Study of Bitumen Recovery by Gravity Drainage Using Low Temperature Solvent Gas Injection. *Cdn. J. of Chemical Engineering* **67** (6): 978–991.

El-Haj, R., Lohi, A. and Upreti, R. 2009. Experimental Determination of Butane Dispersion in Vapor Extraction of Heavy Oil and

Bitumen. *Journal of Petroleum Science and Engineering* 67 (1–2): 41–47.

Jiang, Q. and Butler, R.M. 1995. Experimental Studies on Effects of Reservoir Heterogeneity on VAPEX Process. Paper presented at the 46th Annual Technical Meeting of The Petroleum Society of CIM, Banff, Alberta, 14–17 May.

Knorr, K.D., Wilton, R.R., and Zeng, F.B. 2008. Design and Installation of a High-Pressure 3D Physical Model for Evaluation of Solvent Vapor Extraction Processes. Paper 2008-322 presented at the World Heavy Oil Congress, Edmonton, Alberta, 10–12 March.

Kristoff, B.J., Knorr, K.D., Preston, C.K., Worth, K. and Sawatzky, R. 2008. Joint Implementation of Vapour Extraction Heavy Oil Recovery Process. Paper 2008-468 presented at the World Heavy Oil Congress, Edmonton, Alberta, 10–12 March.

Oduntan, A.R., Chatzis, I., Smith, J., and Lohi, A. 2001. Heavy Oil Recovery using the VAPEX Process: Scale-up Issues. Paper 2001-127 presented at the Petroleum Society's Canadian International Petroleum Conference, Calgary, 12–14 June.

Panda, M.N. and Lake, L.W. 1994. Estimation of Single-Phase Permeability from the Parameters of a Particle-Size Distribution. *AAPG Bulletin* **78** (7): 1028–1039.

Peng, D. Y. and Robinson, D. B. 1976. A New Two Constant Equation of State. *Ind. Eng. Chem. Fundam* **15** (1): 59–64.

Sim, S. and Singhal, A. 2002. Vapex Engineering & Economics, PTRC Joint Industry Project Phase 3: Heavy Oil Recovery in Saskatchewan and Alberta (2002) Vol. 3: Physical Model Experiments.

Upreti, S.R., Lohi, A., Kapadia, A. and El-Haj, R. 2007. Vapor Extraction of Heavy Oil and Bitumen: A Review. *Energy & Fuels* **21** (3): 1562–1574.

Figures

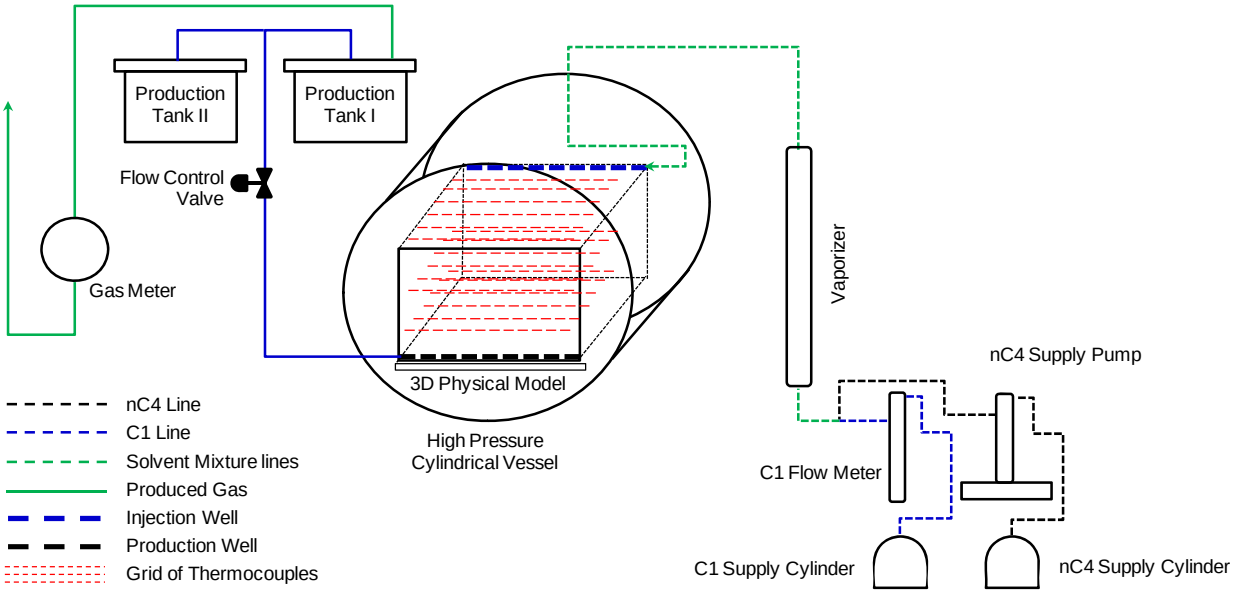

Fig. 1—Schematic of Experimental Setup

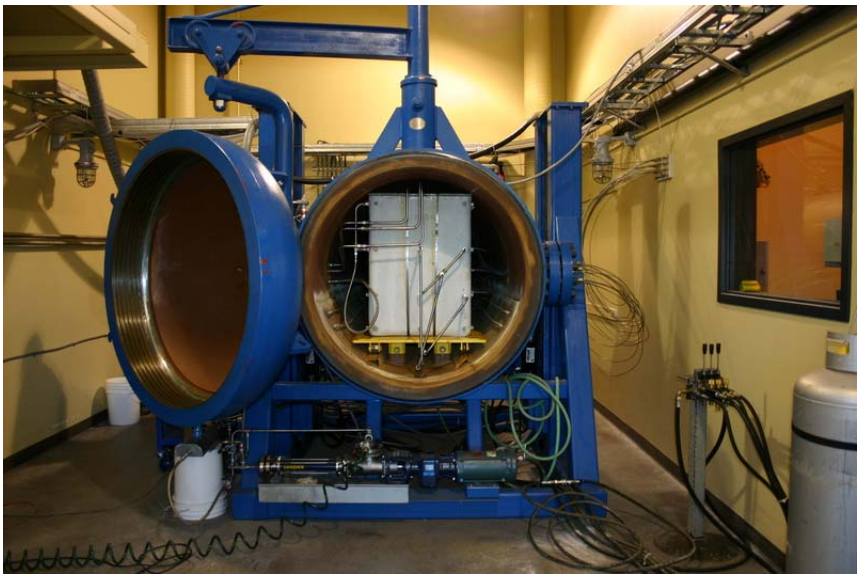

Fig. 2—High Pressure Vessel and 3D Physical Model

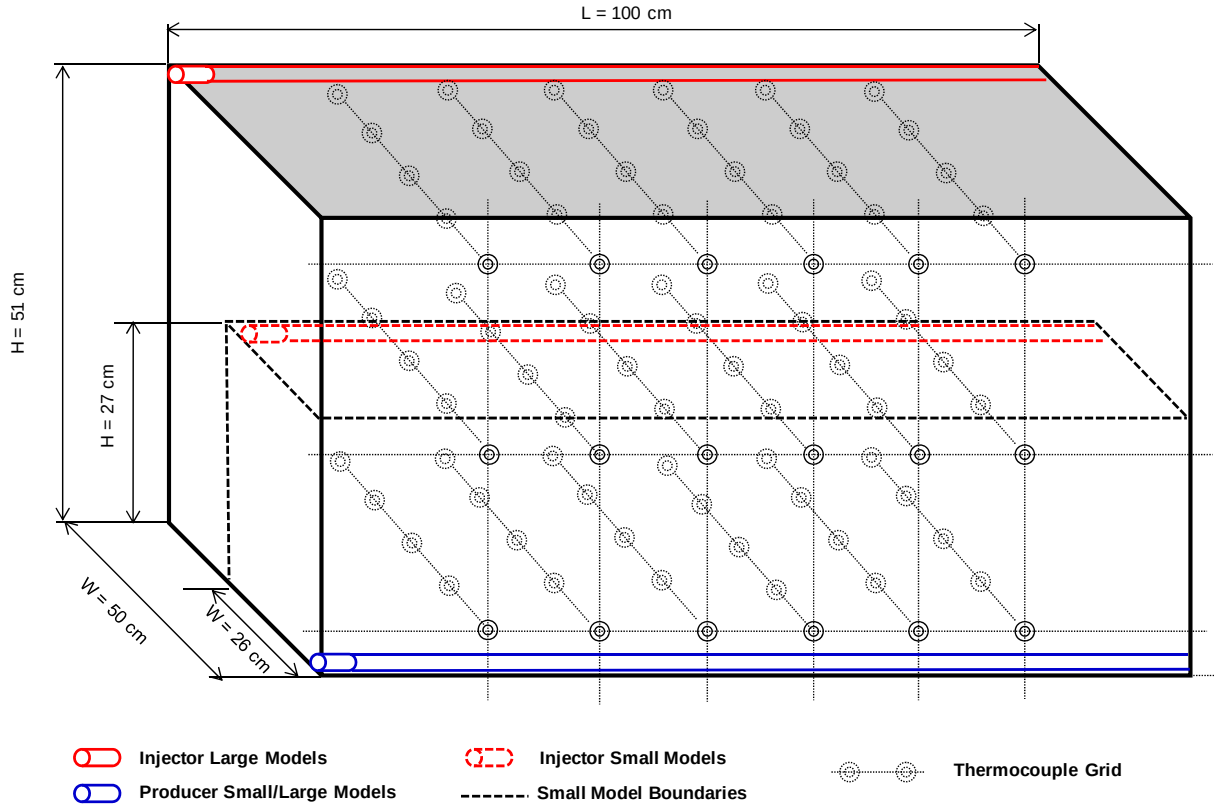

Fig. 3—Thermocouple Grid in Rectangular 3D Model

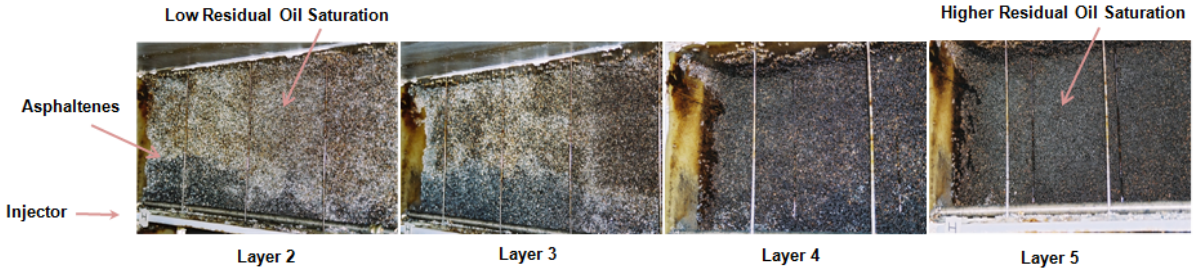

Fig. 4—SVX 1 Model Excavation Results (Four Layers)

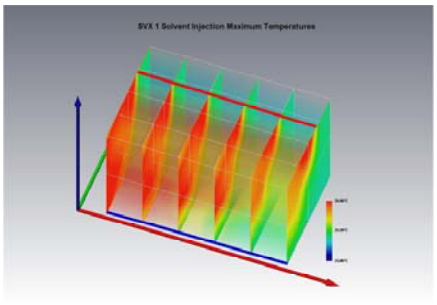

Fig. 5—SVX 1 Solvent Injection Maximum Temperatures

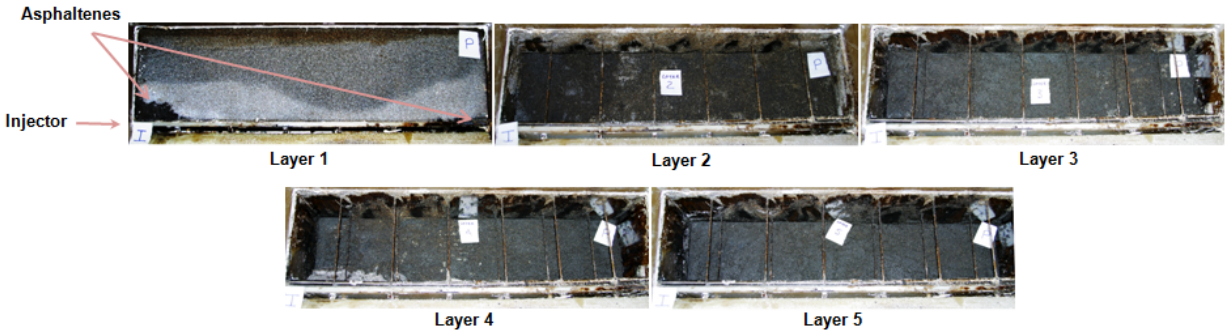

Fig. 6—SVX 2 Model Excavation Results (Five Layers)

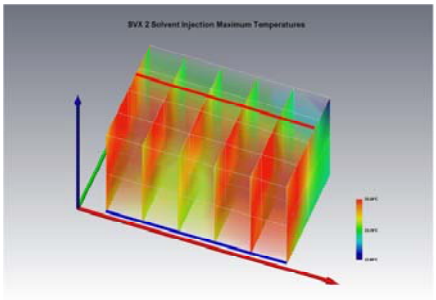

Fig. 7—SVX 2 Solvent Injection Maximum Temperatures

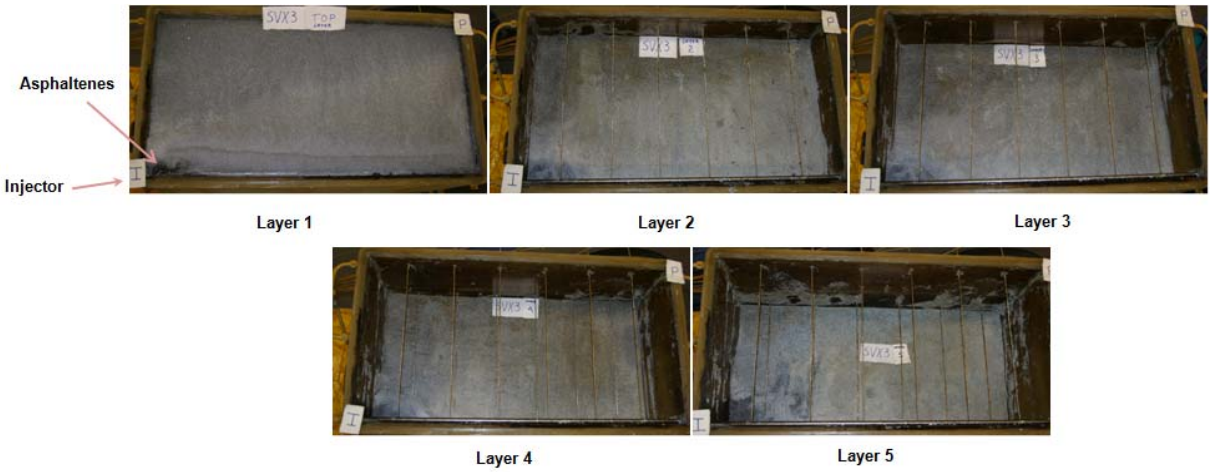

Fig. 8—SVX 3 Model Excavation Results (Five Layers)

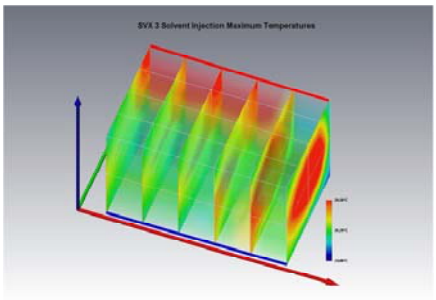

Fig. 9—SVX 3 Solvent Injection Maximum Temperatures

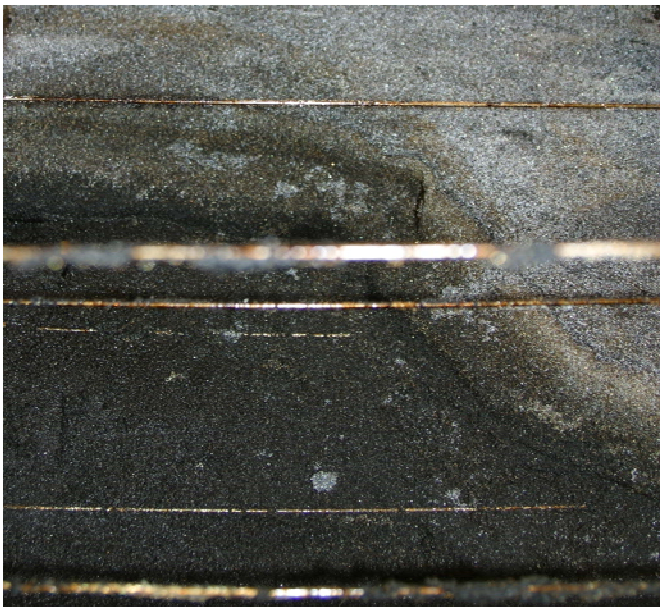

Fig. 10—SVX 3 Model Excavation Solvent/Oil Interface

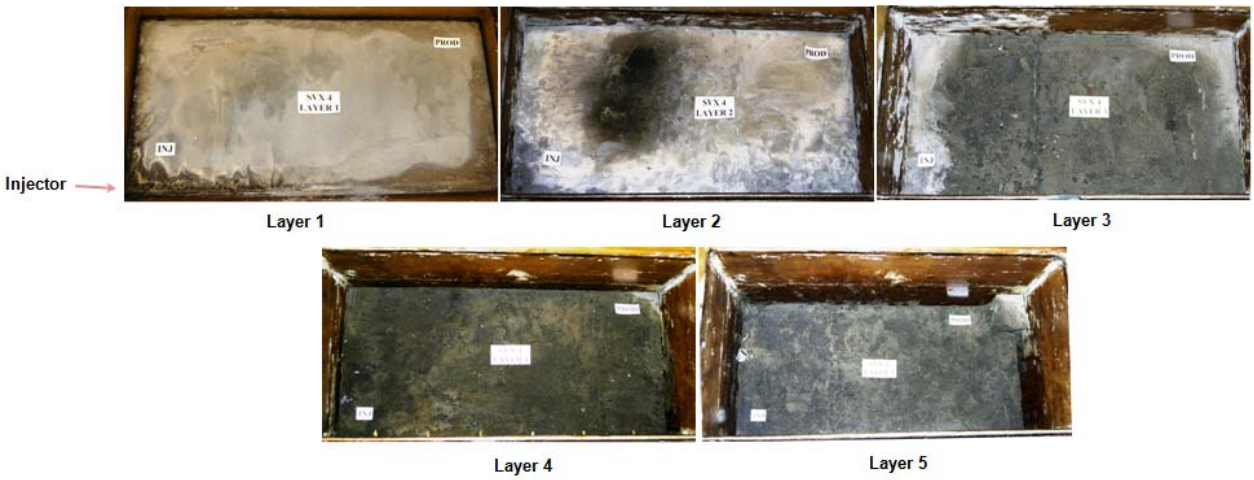

Fig. 11—SVX 4 Model Excavation Results (Five Layers)

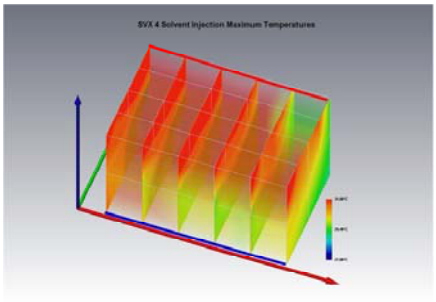

Fig. 12—SVX 4 Solvent Injection Maximum Temperatures

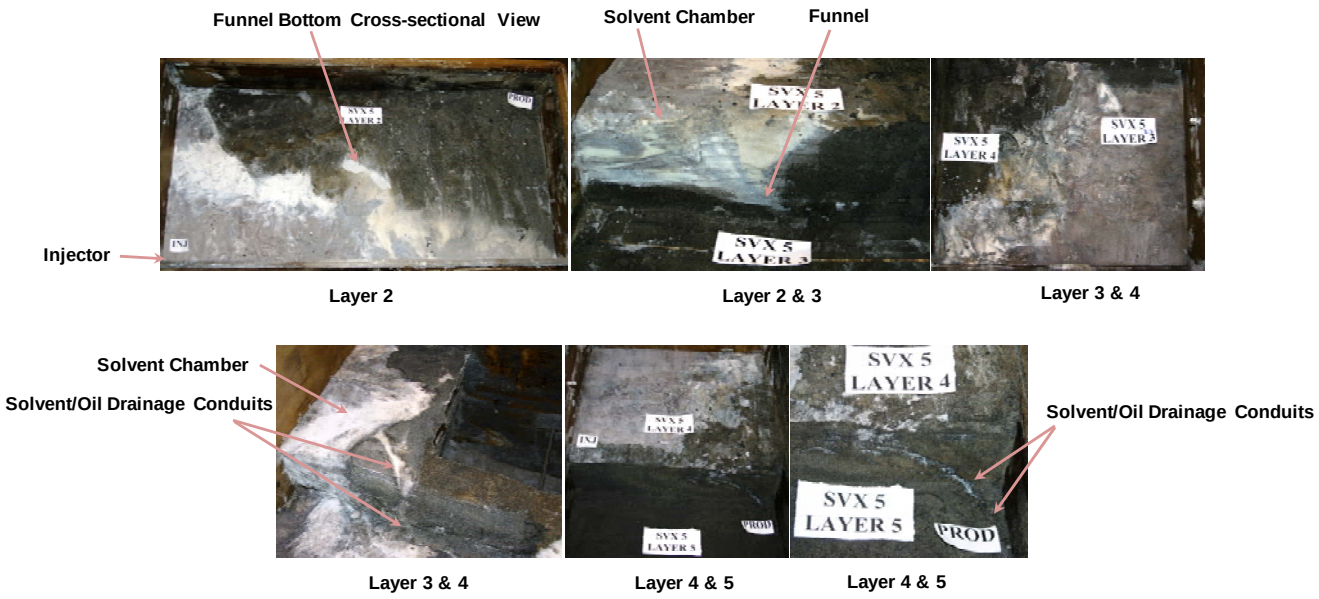

Fig. 13—SVX 5 Model Excavation Results (Five Layers)

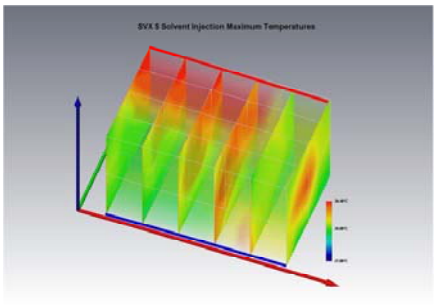

Fig. 14—SVX 5 Solvent Injection Maximum Temperatures

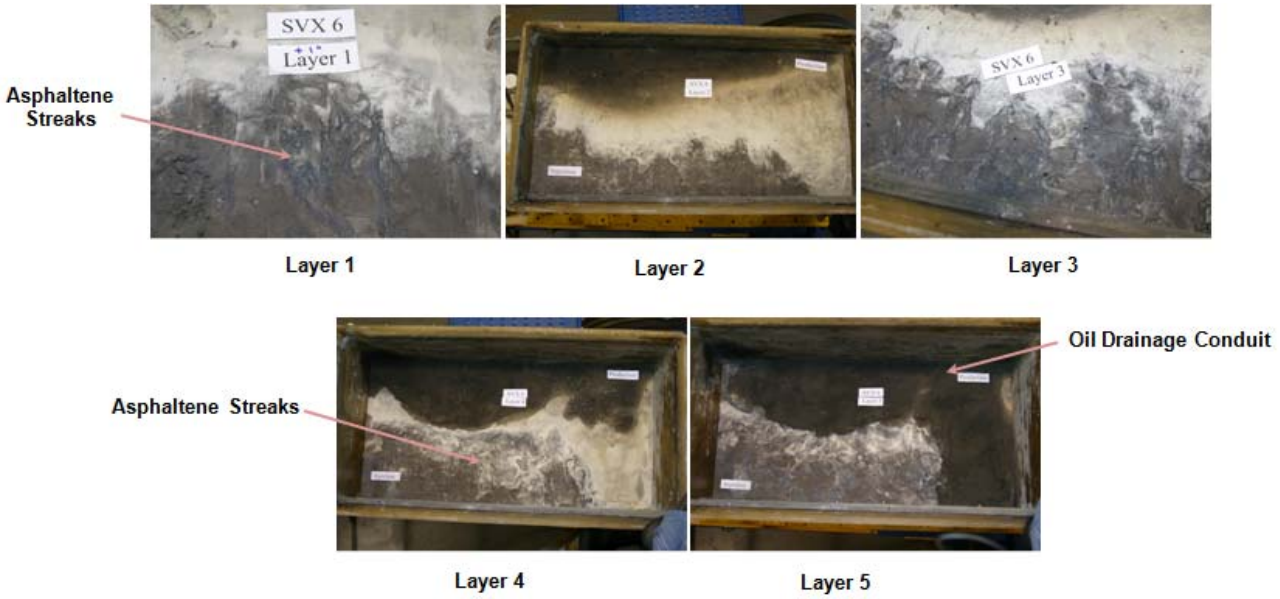

Fig. 15—SVX 6 Model Excavation Results (Five Layers)

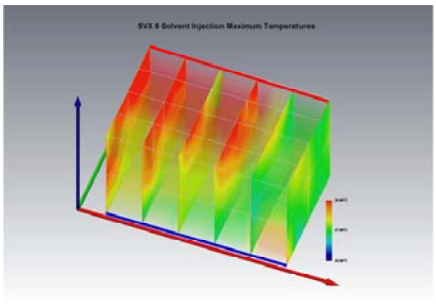

Fig. 16—SVX 6 Solvent Injection Maximum Temperatures

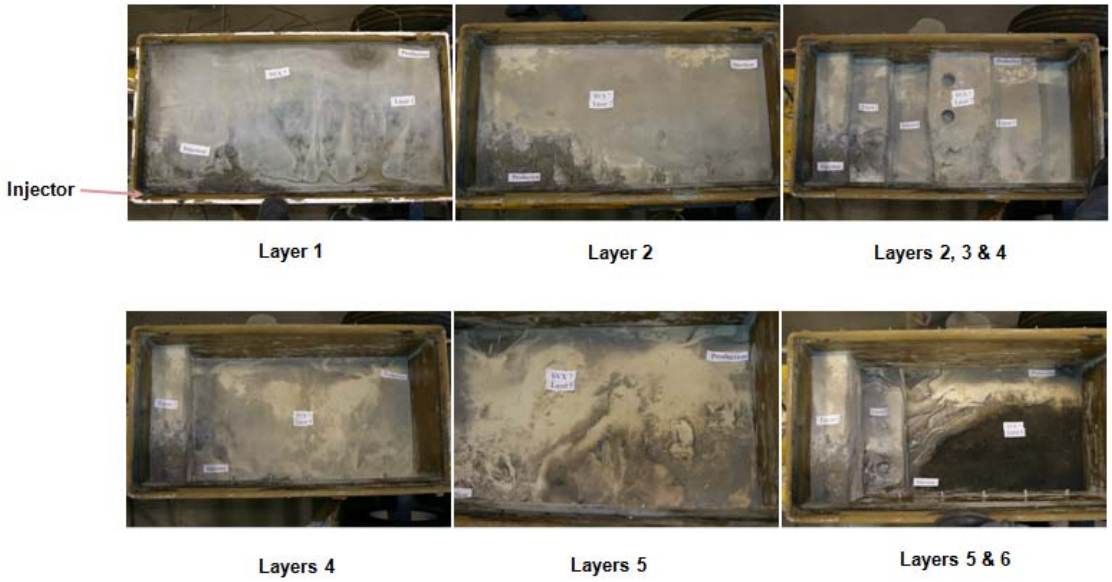

Fig. 17—SVX 7 Model Excavation Results (Five Layers)

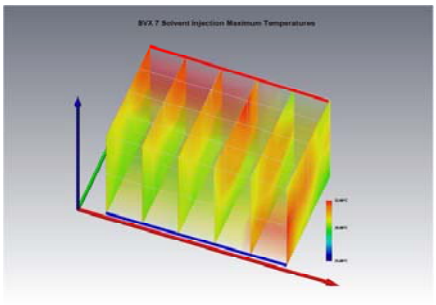

Fig. 18—SVX 7 Solvent Injection Maximum Temperatures

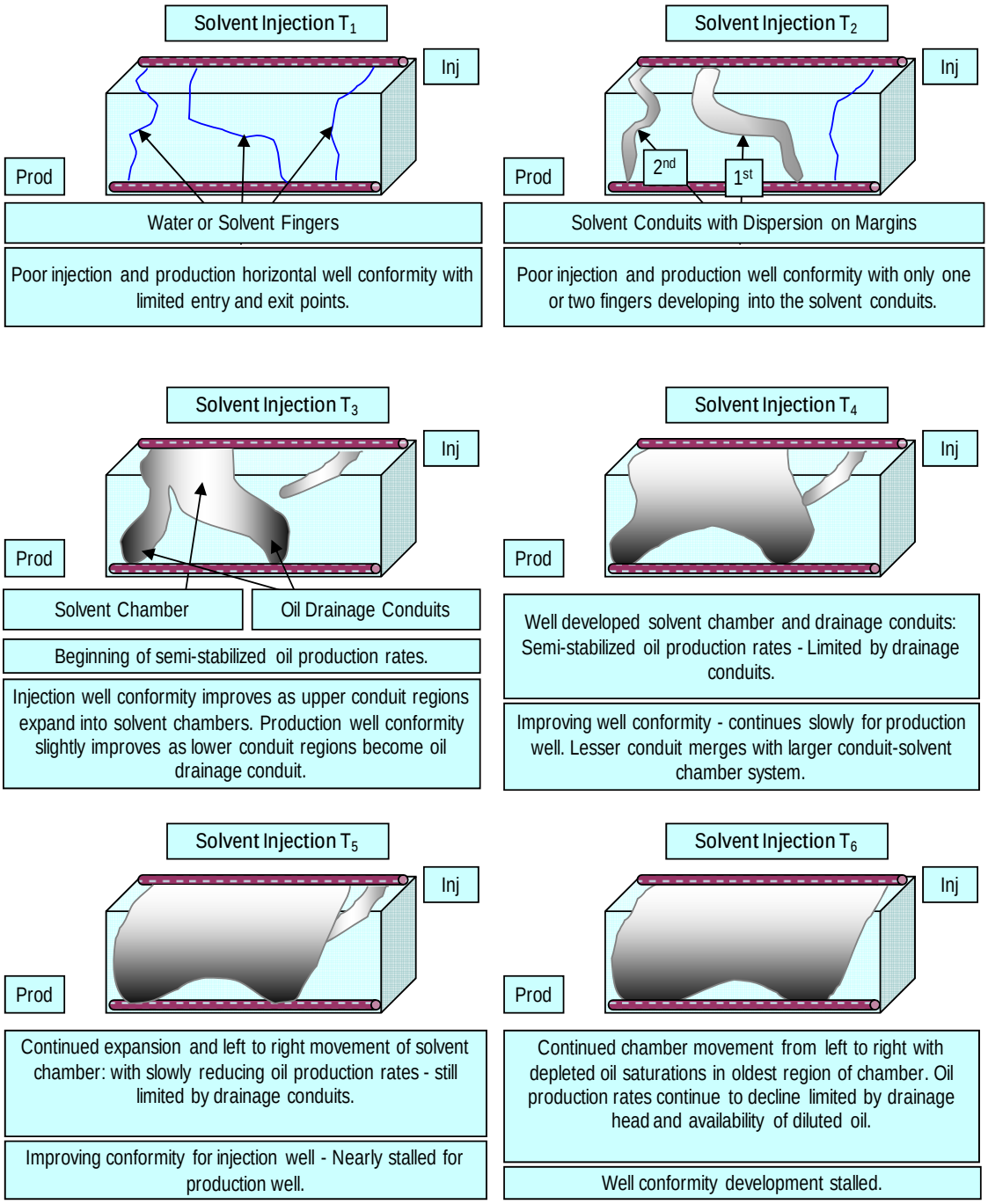

Fig. 19—Solvent and Oil Drainage Conduit Development

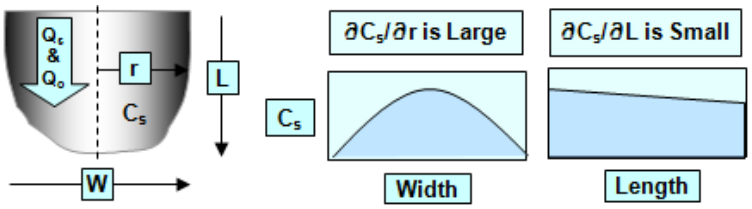

Fig. 20—Solvent Conduit

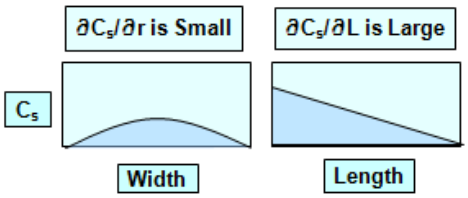

Fig. 21—Oil Drainage Conduit

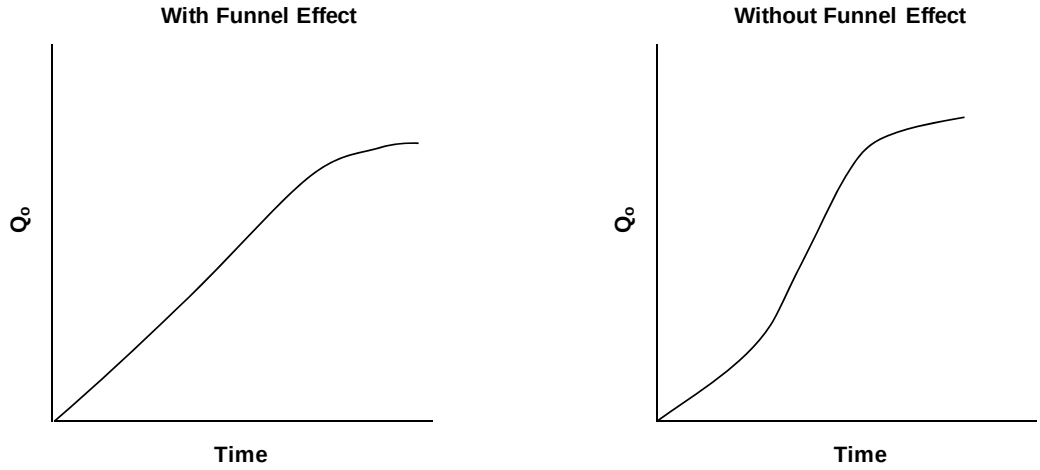

Fig. 22—Oil Production Curves With and Without Funnel Effect

Tables

Table 1—SVX 1 to 7 Run Parameters

Run	Avg Injection Pressure (kPaa)	Model Dimensions L×W×H (cm)	Model Permeability (μm^2)	Model Porosity (%)
SVX 1	314	100×26×27	2,960	37.0
SVX 2	308	100×26×27	301	35.3
SVX 3	311	100×50×51	301	36.3
SVX 4	320	100×50×51	30	36.7
SVX 5	417	100×50×51	8.7	34.8
SVX 6	435	100×50×51	4.1	35.1
SVX 7	317	100×50×51	4.0	35.0

Table 2—SVX 1 to 7 Waterflood Summaries

Run	Time	Initial Saturations		Final Saturations		Oil Recovery	
		Oil	Water	Oil	Water		
	Hours	%PV				Litres	%OOIP
SVX 1	5.10	86.9	13.1	85.5	14.5	0.35	1.52
SVX 2	4.93	84.9	15.1	79.5	20.5	1.37	6.33
SVX 3	17.9	93.9	6.1	79.6	20.4	13.2	15.2
SVX 4	19.8	92.0	8.0	82.0	18.0	9.40	10.9
SVX 5	18.3	96.8	3.2	72.9	27.1	21.6	24.7
SVX 6	17.3	97.2	2.8	74.9	25.1	20.2	22.9
SVX 7	24.0	96.7	3.3	74.1	25.9	20.6	23.4

Table 3—SVX 1 to 7 Solvent Injection Summaries for 0.212 kg/L PV Solvent Injected

Run	Time	Initial Saturations		Final Saturations			Solvent Injected Below DP	Solvent Retention	Oil Recovery	
		Oil	Water	Oil	Water	Gas				
	Hours	%PV					% Inj Time	% Kg Inj	L/day	%OOIP
SVX 1	6.98	85.5	14.5	40.9	5.26	53.8	100	33.7	41.7	51.3
SVX 2	6.64	79.5	20.5	56.9	7.45	35.6	100	32.2	20.8	26.6
SVX 3	24.1	79.6	20.4	51.9	10.5	37.5	100	22.2	25.3	29.4
SVX 4	24.6	82.0	18.0	72.5	12.3	15.2	80.0	15.4	8.78	10.4
SVX 5	23.5	72.9	27.1	54.0	9.91	36.1	63.2	48.8	17.4	19.5
SVX 6	23.6	74.9	25.1	61.0	7.29	31.7	0.00	53.1	12.9	14.3
SVX 7	23.7	74.1	25.9	54.8	11.6	33.6	92.7	27.8	17.7	19.9

Table 4—SVX 1 to 7 Solvent Injection Summaries for Total Injection Time

Run	Time	Initial Saturations		Final Saturations			Solvent Retention	Oil Recovery	
		Oil	Water	Oil	Water	Gas			
	Hours	%PV					% Kg Inj	L/day	%OOIP
SVX 1	6.98	85.5	14.5	40.9	5.26	53.8	33.7	41.7	51.3
SVX 2	6.94	79.5	20.5	55.9	6.80	37.3	27.5	20.8	27.6
SVX 3	68.2	79.6	20.4	18.8	6.50	74.7	12.0	19.8	64.8
SVX 4	65.6	82.0	18.0	60.9	5.47	33.6	9.74	7.23	22.9
SVX 5	42.9	72.9	27.1	49.1	8.70	42.2	43.4	12.0	24.5
SVX 6	108	74.9	25.1	46.1	1.71	52.2	24.4	5.82	29.6
SVX 7	202	74.1	25.9	13.9	3.04	83.0	10.1	6.49	62.2